6-2021

Microfluidic-Assisted Fabrication of Reverse Micelle/PLGA Hybrid Microspheres for Sustained Vascular Endothelial Growth Factor Delivery

Meisam Omidi
Marquette University

Luis Eduardo Almeida
Marquette University, luis.almeida@marquette.edu

Lobat Tayebi
Marquette University, lobat.tayebi@marquette.edu

Biotechnology and Applied Biochemistry, Vol. 68, No. 3 (June 2021): 616-625. DOI.

Microfluidic-Assisted Fabrication of Reverse Micelle/PLGA Hybrid Microspheres for Sustained Vascular Endothelial Growth Factor Delivery

Meisam Omidi
Marquette University School of Dentistry, Milwaukee, WI
Luis Almeida
Marquette University School of Dentistry, Milwaukee, WI
Lobat Tayebi
Marquette University School of Dentistry, Milwaukee, WI

Abstract

In this study, poly (d, l-lactide-co-glycolide) (PLGA) composite microspheres containing anhydrous reverse micelle (R.M.) dipalmitoylphosphatidylcholine (DPPC) nanoparticles loaded vascular endothelial growth factor (VEGF) were produced using microfluidic platforms. The VEGF-loaded R.M.

nanoparticles (VRM) were achieved by initial self-assembly and subsequent lipid inversion of the DPPC vesicles. The fabricated VRMs were encapsulated into the PLGA matrix by flow-focusing geometry microfluidic platforms. The encapsulation efficiency, *in vitro* release profile, and the bioactivity of the produced composite microspheres were investigated. The release study showed that VEGF was slowly released from the PLGA composite microspheres over 28 days with a reduced initial burst (18 ± 4.17% in the first 24 H). The VEGF stability during encapsulation and release period was also investigated, and the results indicated that encapsulated VEGF was well preserved. Also, the bioactivity assay of the PLGA composite microspheres on human umbilical vein endothelial cells was confirmed that the encapsulated VEGF was utterly active. The present monodisperse and controllable VEGF-loaded microspheres with reproducible manner could be widely used in tissue engineering and therapeutic applications.

1 Introduction

Nowadays, biopharmaceuticals product include proteins such as growth factor have been used vastly in the clinic treatment [1, 2]. However, proteins generally are very sensitive macromolecules, and their functionality can be affected by external conditions. Moreover, short half-lives of proteins are known as another critical issue in the maintenance of their effective therapeutic concentration [3]. On the other hand, the current biopharmaceuticals product are commonly used in the long-term treatment of chronic diseases [4]. Consequently, the application of drug delivery systems for long-term protein delivery can significantly improve treatment quality [5].

The formation of a functional vascular network is a key factor in tissue repair and regeneration [6]. During past decades, the physiological mechanisms involved in the vascularization process have been extensively investigated [7, 8], and vascular endothelial growth factor (VEGF) has been identified as one of the critical regulator's factors in neovascularization. The potential use of VEGF, particularly in the vascular restoration of injured and ischemic tissues, has been indicated in the literature [9-11]. Despite the therapeutic benefits of VEGF via angiogenesis and vasculogenesis, its excessive amounts of exposure can lead to deleterious outcomes. VEGF has been implicated in a wide verity of the disease such as diabetic retinopathy [12], non-Hodgkin's lymphoma, multiple myeloma, and acute/chronic leukemia [13]. Furthermore, excessive amounts of VEGF can aid tumor growth and intensely increase the risk of tumorigenesis [14, 15]. In addition to the biosafety issues, direct injection or seeding of VEGF into the target site has been not a cost-effective approach owing to its short half-life. As a result, the application of VEGF in a specific treatment or regenerative process entirely relies upon accurate control over the kinetic profiles of it in a target area [7]. Consequently, the need to develop the new delivery approaches of VEGF to the specific site has attracted the attention of several research groups [16, 17]. However, these propose approaches unable to address many key issues, including tissue targeting tunable release rates and low systemic exposure [9, 10, 13].

Highlights

- PLGA composite microspheres containing anhydrous reverse micelle nanoparticles loaded VEGF were produced using microfluidic platforms.
- The release study showed that VEGF was slowly released from the PLGA composite microspheres over 28 days with a reduced initial burst.

- The VEGF stability during encapsulation and release period was well preserved.

Among the available biomaterials, biopolymers such as poly (d, l-lactide-co-glycolide) (PLGA) are promising options that can be used for the development of long-term protein delivery systems [18]. PLGA, as one of the United States Food and Drug Aadministration approved biopolymers, has been applied for developing therapeutic devices in recent years [19-23]. Due to the unique chemical, physical, and mechanical properties, as well as excellent biocompatibility and adjustable biodegradability properties, PLGA is known as an attractive candidate for VEGF delivery [24]. However, strong hydrophobic characteristics of PLGA has to be considered [18]. However, strong hydrophobic characteristics of PLGA have to be considered [18]. This hydrophobic property can lead to deleterious outcomes in protein-loaded PLGA microspheres such as low encapsulation efficacy and minimizing initial burst release, which increases potential risks in the initial period [21, 23].

Owning to its rapid and straightforward preparation procedure, double emulsion techniques are conventional approaches to produce protein-loaded PLGA microspheres [24]. However, the resulting PLGA microspheres from double emulsion techniques are highly polydisperse particles. As a result, the different release profiles can be presented by the polydisperse protein-loaded microspheres [25]. The microfluidic technique is generally used to produce monodisperse PLGA microspheres in a highly controllable and reproducible manner [26]. The on-chip-based approaches have been extensively utilized to encapsulate different biomolecules and drugs [25-27]. However, many critical issues in the fabrication of proteins-loaded microspheres are remained [27].

The present study aimed to develop PLGA composite microspheres containing anhydrous reverse micelle (R.M.) dipalmitoylphosphatidylcholine (DPPC) nanoparticles-loaded VEGF by microfluidic platforms to protect VEGF bioactivity and reduce the initial burst release. The VEGF-loaded R.M. (VRM) nanoparticles were achieved by initial self-assembly and subsequent lipid inversion of the DPPC vesicles. The fabricated VRMs were encapsulated into the PLGA matrix by flow-focusing geometry microfluidic platforms. The produced composite microspheres were fully characterized and release profile, and bioactivity of the loaded VEGF was also described.

2 Materials and Methods

2.1 Materials

Vascular endothelial growth factor-A(165) was purchased from Cell Applications (CA , USA). PLGA (75:25, Mw 76,000–115,000, a viscosity of 0.7 dL/g), human VEGF ELISA assay kit, endothelial cell growth medium 2 supplement, dichloromethane (DCM), and cell proliferation reagent WST kit were purchased from Sigma–Aldrich (WI, USA). 1,2-Dipalmitoyl-sn-glycero-3-phosphocholine was obtained from Avanti Polar (AL, USA). Polyvinyl alcohol (Mw 500–5,000) was gained from VWR (CO, USA).

2.2 Preparation of VRM nanoparticles

The VEGF-loaded DPPC nanoparticles were fabricated by the bottom-up method. Briefly, VEGF was dissolved in phosphate-buffered saline (PBS) (2 mg/mL) to form the aqueous phase, whereas DPPC was dissolved in DMSO (50 mg/mL). Subsequently, a 1 mL DPPC solution was added to 4 mL of the aqueous phase dropwise under stirring at 1,000 rpm for 20 Min at 37.0 °C. The resulting mixture was frozen and lyophilized.

2.3 Production of the VRM-loaded microspheres

In this study, VRM-loaded PLGA microspheres (VMPs) were prepared by the microfluidic droplet approach. The droplets fluid or S/O phase (VEGF and PLGA solution) was obtained by solving 50 mg of PLGA, 0.1 mg VRM or native VEGF, and 1 mg Mg $(OH)_2$ in 5 mL (DCM). The mixture was vortexed and sonicated for 30 Sec. The carrier fluid or continuous phase was prepared by solving 500 mg PVA in a 25 mL water. To remove large particles, the droplets and carrier fluid was filtered by 0.2 µm filtrate. The fluids were transferred to 3D flow focusing droplet chip 100 µm hydrophilic (Part No. 3200433; Dolomite, UK) microfluidic chip by syringe pumps through FEP tubes (Fig. **1**). The chip outlet was collected in 100 mL of PVA solutions (2% wt% in PBS) and continuously stirred at 200 rpm. The VRM-loaded microspheres were lyophilized after centrifuged and washed with DI water.

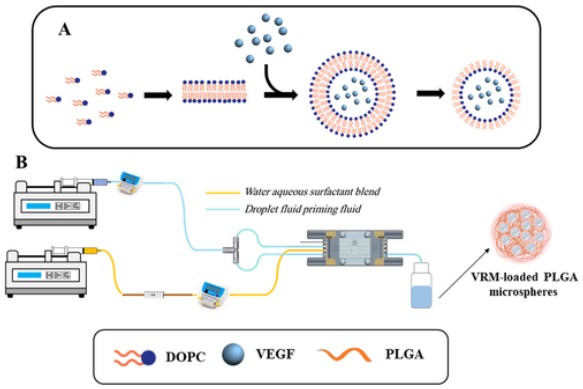

FIG. 1 Schematic representation of (A) VRM nanoparticle fabrication and (B) the microfluidic setup for VRM-loaded PLGA microspheres (VMPs) production.

2.4 Encapsulation efficiency

The amount of VEGF actual loading in PLGA microspheres was calculated by the degradation of 10 mg of the VMPs in 2 mL of 0.1 N NaOH. After 8 H, the mixtures were centrifuged (4000 g, 10 Min) and the supernatant was collected. ELISA assay kit was used to measure the VEGF content in this solution. The loading efficiency was calculated by the ratio of actual to theoretical loading × 100 ± standard deviations. The standard deviation value was defined by repeating this test for five different samples.

2.5 *In vitro* release

For the *in vitro* release, 10 mg of VRM-loaded PLGA microspheres suspended in 1 mL PBS (1× pH 7.4)) and incubated in a shaker incubator at 37.0 °C at 100 rpm. At predetermined time intervals, the samples were centrifuged (6,000 rpm, 10 Min), and the **supernatants** were replaced with the fresh PBS. The VEGF concentration in the collected samples was measured by ELISA assay kits.

2.6 VEGF bioactivity assay

Bioactivity of the VEGF released from VRM-loaded PLGA microspheres was evaluated using an assay measuring the proliferation of human umbilical vein cells (HUVECs) (ATCC® PCS100-013™). The HUVECs were expanded in T-25 cell culture flasks by endothelial cell growth medium-2 containing all necessary supplements and growth factors such as recombinant insulin-like growth factor, basic fibroblast growth factor, epidermal growth factor, VEGF, heparin, ascorbic acid, and hydrocortisone with 5% fetal bovine serum, and 1% streptomycin/penicillin. The cells were incubated at 37 °C and 5% CO_2. The effect of cell

number and culture medium on HUVEC proliferation assays was investigated, and optimized conditions for the bioactivity assay were obtained. The pilot study showed that culture 2,000 cells per well in the base medium contains serum only was the optimal condition for the bioactivity assay VEGF on HUVEC.

To perform the proliferation assay, 2×10^3 HUVECs were seeded in each well of 96-well plates using the base medium supplemented with 5% fetal bovine serum and 1% streptomycin/penicillin. After 24 H, the HUVECs were treated with 1 µg of VEGF-loaded or VRM-loaded PLGA microspheres (eight wells per group). Native VEGF (at the same concentrations corresponding to the released volume added daily) and PBS were used as positive and negative controls, respectively (eight wells per group). Number of cells in each treatment group was measured after 1, 2, 3, 5, and 8 days using metabolic WST-1 assay. In brief, 10 µL WST-1 reagent was added to each well and the plates were incubated in humidified atmosphere containing 5% CO_2 at 37 °C for 4 H. Then, the light absorbance was measured at 600 nm [28, 29].

Moreover, the potential of released VEGF from VRM-loaded PLGA microspheres to stimulate cellular responses by binding to VEGF receptor 2 (VEGFR2/KDR) was evaluated by the VEGF Bioassay kit (Promega® GA2001). In brief, the KDR/NFAT-RE HEK293 cells were treated by VRM-loaded PLGA microspheres. Then, the NFAT-RE-mediated luminescence induced by activation of KDR was measured by a luminometer after 3 days [30]. All experiments were replicated three times.

2.7 Characterization

The JEM-1400 transmission electron microscopy morphology (TEM) was used to examine VEGF-loaded DPPC nanoparticles. The size distribution of the VEGF-loaded DPPC nanoparticles sample was measured by Malvern ZEN 3600 dynamic light scattering (DLS) analysis. Briefly, 50 µL of VRM was diluted in 3 mL of PBS (1×, pH 7.4), and the sample was transferred to cuvet for DLS analysis. Hydrodynamic diameter size distribution was measured five times at room temperature. The size and microstructure of PLGA VMPs were studied by LEXT OLS4000 3D laser measuring microscope. The image analysis method that described previously was used to calculate the size of PLGA VMPs [28, 29]. Briefly, for each sample, three different images were captured and processed by ImageJ software (ImageJ freeware; NIH, USA). Circular dichroism (CD) spectroscopy (Applied Photophysics Ltd.) was used to study the secondary structure of the VEGF extracted from VEGF and VRM-loaded PLGA microspheres. The collected released VEGF from the microspheres was transferred into a 1.0 mm path length quartz cuvette, and CD spectra of each sample were recorded at a wavelength range of 190–250 nm.

3 Results and Discussion

The size and morphology of VEGF-loaded DPPC and VRM nanoparticles in DCM were investigated by TEM and DLS analysis (Figs. **2A–2D**). As present in Fig. **2A**, the synthesized VEGF-loaded DPPC nanoparticles have irregular shapes with an average particle size of around 160 nm, whereas VRM nanoparticles showed a relatively small particle size of approximately 90 nm (Fig. **2B**). Also, the hydrodynamic diameter of synthesized VEGF-loaded DPPC and VRM nanoparticles was 239 ± 15 and 150 ± 15 nm, respectively. The lipid inversion theory can be used to explain the mechanisms of VRM nanoparticle formation during the lyophilization process [31]. Briefly, the protein-loaded DPPC lipid bilayers nanoparticles were produced based on self-assembly of amphiphilic DPPC molecules with a

fraction of dissolved VEGF. The VEGF can be existed simultaneously inside and outside of lipid vesicles. Because of phase separation and solvent evaporation during the lyophilization process, anhydrous nuclei were initially formed. The produced nuclei contained cryoprotectants and proteins. Subsequently, DPPC hydrophilic head groups accumulated onto the surface of the nuclei. By introducing organic solvent (DCM), DPPC hydrophobic tails around the nuclei dispersed and stretched in the organic solvent. On the other hand, owning to hydrophilic interaction of protein and DPPC hydrophilic head, DPPC absorbed on the surface of nuclei, and VRM nanoparticles were formed. In the produced VRM nanoparticles, VEGF was encapsulated in R.M., and it can be homogeneously dispersed in the organic solvent because of hydrophobic tails [31]. The R.M. could effectively protect the VEGF against organic solvents and preserve protein activity and stability during PLGA microspheres fabrication.

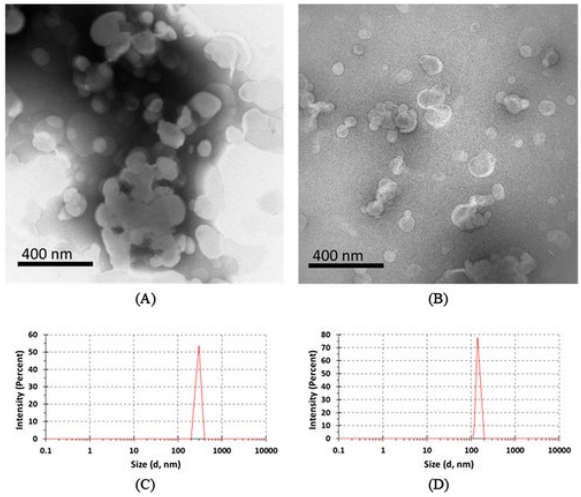

FIG. 2 TEM micrographs of (A) VEGF-loaded DPPC and (B) VRM nanoparticles in the DCM. Hydrodynamic diameter of (C) synthesized VEGF-loaded DPPC and (D) VRM nanoparticles.

The VRM-loaded PLGA microspheres were achieved by initial in chip droplets formation and subsequent solvent extraction from droplets. The effect of carrier (C_f) and droplet flow rate (C_d) on the formation of the PLGA droplets is presented in Fig. **3**. The typical image of the droplet formation in the microfluidic chip is shown in Figs. **3A** and **3B**. According to Figs. **3A** and **3B**, the droplet sizes and generation frequency rates were changed by increasing C_f. The droplet size and frequency of the droplet formation for different values of C_f and C_d are shown in Figs. **3C** and **3D**, respectively. The generation frequency rate of droplet formation is defined by the ratio of C_d to the volume of the droplet. Based on Figs. **3C** and **3D**, the PLGA droplets with a size range of 32–101 µm and the generation frequency rate range of 0.1–14 kHz are obtained in the present microfluidic platform.

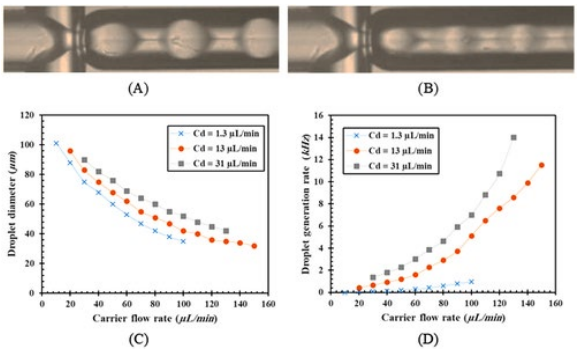

FIG. 3 (A) PLGA droplets formation in X-junction chip at (A) C_f = 20 µL/Min, C_d = 1.3 µL/Min, and (B) C_f = 80 µL/Min, C_d = 1.3 µL/Min. (C) Droplet diameter and (D) droplet generation rate for different values of carrier flow rate (C_f) and droplet flow rate (C_d).

In order to form VRM-loaded PLGA microspheres, the solvent (DCM) should be extracted from the droplet. The size and morphology of VRM-loaded PLGA microspheres were studied by a 3D laser microscope (Figs. **4A–4D**). Figures **4A–4D** show that the VRM-loaded PLGA microspheres are highly monodisperse in size (CV < 3%). According to the droplet size, the PLGA microsphere's size can be varied from 14 to 39 µm.

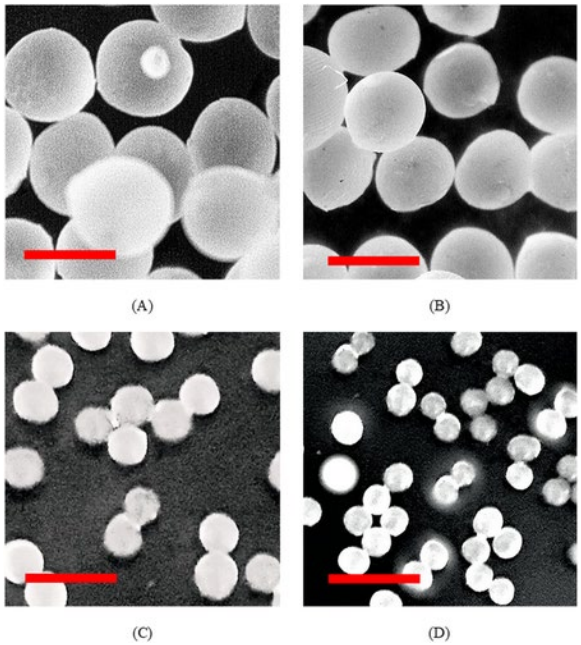

FIG. 4 Micrographs of VRM-loaded PLGA microspheres (A) C_f = 10 µL/Min, C_d = 1.5 µL/Min, (B) C_f = 30 µL/Min, C_d = 1.5 µL/Min, (C) C_f = 80 µL/Min, C_d = 1.5 µL/Min, and (D) C_f = 100 µL/Min, C_d = 1.5 µL/Min (scale bar = 40 µm).

The loading efficiency of native VEGF and VRM in the PLGA microspheres with different particles size was presented in Fig. **5A**. Owning to microspheres size, encapsulation efficiency of the prepared microspheres was varied from 78% to 93% and 19% to 39% for VRM and native VEGF, respectively. The significant difference in loading efficiency for native VEGF and VRM could be attributed to the drug migration rates [31, 32]. During the droplet formation and solvent extraction process, VEGF tended to escape to the external water phase due to its hydrophilic properties. In contrast, the drug migration

could effectively prevent by hydrophobic properties of encapsulating VEGF into R.M. nanoparticles. Consequently, a much higher loading efficiency was achieved by VRM in comparison with native VEGF. Also, the encapsulation efficiency of proteins could be described as a function of microspheres particle size. Generally, the highest protein loading efficiency, which has been reported in the literature, is around 60% for similar particle sizes[33-36].

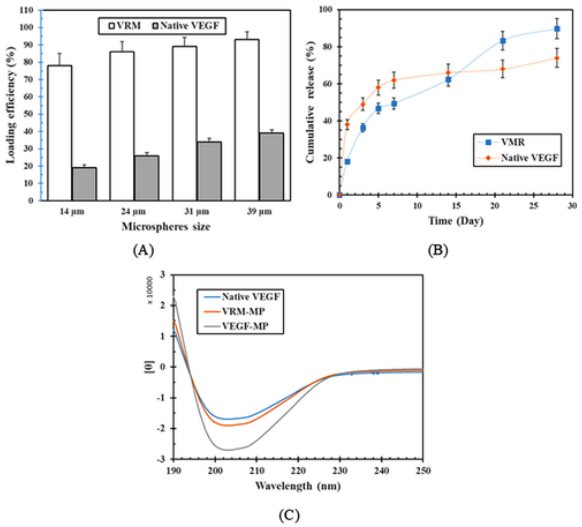

FIG. 5 (A) The loading efficiency of native VEGF and VRM-loaded PLGA microspheres. (B) Release profiles of VEGF released from PLGA microspheres in PBS (pH 7.4). (C) Far-UV CD spectra of native VEGF solution and VEGF extracted from VEGF and VRM-loaded PLGA microspheres.

The *in vitro* release profiles of VEGF and VRM-loaded PLGA microspheres were shown in Fig. **5B**. The release of drug molecules from PLGA microparticles can happen from three possible ways (i) transport through the polymer, (ii) because of the encapsulating polymer dissolution, and (iii) transport through water-filled pores. In the case of too hydrophilic and too large biopharmaceutical such as a peptide or a protein, transport through water-filled pores is a major way of release. Diffusion and convection are two common ways of transport in transport through water-filled pores mechanism [32]. In contrast, transport through the polymer phase is a more convenient way of release for hydrophobic and small drugs. PLGA in aqueous media can swell by absorbing water due to its mobile polymer chains. The internal pressure of the polymer can increase water absorption, and this pressure can be probably compensated by rearrangement of the polymer chains and swelling [37]. However, before the drug being released, it must enter the aqueous phase, either in the inside pores or at the surface. Native VEGF-loaded PLGA microspheres exhibited initial burst release (38 ± 5.43% in the first 24 H). After this burst release, the slow and sustainable release profile (29% ± 4.43% in the 1–28 days) observed for native VEGF-loaded PLGA microspheres.

The VEGF was released from PLGA microspheres by diffusion through water-filled pores. In the initial phase, the burst release can be attributed to nonencapsulated VEGF on the surface or the molecules close to the surface of microspheres. The accumulation of VEGF at the surface of microspheres can be described by hydrophilic neuter of proteins. Similar results for VEGF and other proteins have been reported in other studies [31, 32]. In contrast, VRM-loaded PLGA microspheres showed zero-order controlled release with a highly reduced initial burst (18 ± 4.17% in the first 24 H). The uniform

distribution of drugs in PLGA microspheres is one of the most important factors in decrease initial burst release. As presented in Table **1**, initial burst release was observed for vast verity drugs such as VEGF, lysozyme, and piroxicam. A significant reduction of initial burst release of VEGF in VRM-loaded PLGA microspheres could be related to good dispersion of VEGF in the microspheres [31, 32]. As mention above, the uniform VEGF distribution into the PLGA microspheres was improved by encapsulating VRM nanoparticles. Also, the formation of aggregated unreleasable VEGF was prevented by using VRM [33].

TABLE 1. Drug release from PLGA microparticles in the first 24 H

Drug	Polymer/copolymer	Size	Release amount after 24 H (%)	Ref.
VEGF	50:50 PLGA copolymer	200–600 nm	42%	38
VEGF	50:50 PLGA copolymer	10–60 μm	48%	39
VEGF	50:50 PLGA copolymer	6.61 ± 0.35 μm	38%	40
	50:50 PLGA copolymer (5% PEG)		64%	
VEGF	50:50 PLGA copolymer	2.1–205 μm	64%	41
lysozyme	50:50 PLGA copolymer	0.2–6.5 μm	52%	42
Piroxicam	50:50 PLGA copolymer	10–50 μm	68%	43
Ibuprofen	50:50 PLGA copolymer	24–141 μm	28%	44
5-Fluorouracil	50:50 PLGA copolymer	36–56 μm	21%	45

Far-ultraviolet CD spectroscopy was used to study the secondary structure of VEGF extracted from the microspheres (Fig. **5C**). The CD spectrum of native VEGF shows an intense dichroic band around 190 nm and a broad negative band between 200 and 208 nm, which associated with β-sheets and α-helical structure [32]. Although the extracted VEGF from the VRM-MP depicted almost identical spectra to the native VEGF, the CD spectra of the VEGF-MP showed more significant changes. This result indicated that the secondary structure of encapsulated VEGF was more preserved in the VRM-MP sample.

The biological activity of native VEGF- and VRM-loaded PLGA microspheres was investigated by HUVEC proliferation assay and VEGF bioassay using KDR/NFAT-RE HEK293 cells (Fig. **6**). As shown in Fig. **6A**, native VEGF-loaded microspheres (5 μg/mL) induced a 1.15, 1.18, 1.2, 1.22, and 1.23 fold increase in HUVEC proliferation in comparison with the control group after 1, 2, 3, 5, and 8 days ($P < 0.05$). However, VRM-loaded microspheres induced HUVECs proliferation significantly higher than control and native VEGF-loaded microspheres (1.1, 1.2, 1.3, 1.35, and 1.43 fold increase at 1, 2, 3, 5, and 8 days in culture ($P < 0.01$), respectively). A similar increase in HUVECs proliferation was also observed in cells treated with native VEGF ($P < 0.01$; Fig. **6A**). Furthermore, the VEGF bioassay was used to evaluate the bioactivity of released VEGF, as assessed by activation of the KDR receptor signaling pathway. The NFAT-RE-mediated luminescence induced by activation of KDR was increased by 18.31, 15.77, and 21.64 folds after treatment of KDR/NFAT-RE HEK293 cells with VRM-loaded microspheres, native VEGF-loaded microspheres, and native VEGF ($P < 0.05$; Fig. **6D**). This result indicates that the VEGF

biofunctionality was preserved by R.M. nanoparticles. However, the biofunctionality of native VEGF was attenuated during the encapsulation process in native VEGF-loaded PLGA microspheres.

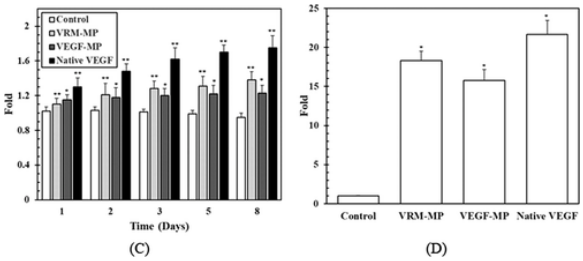

FIG. 6 (A) The proliferation of HUVECs treated with native VEGF (10 ng/mL) or the same concentration of VRM-MP and VEGF-MP (25 ng/mL) in comparison with control group (culture medium alone). (B) KDR activation assay of native VEGF solution and VEGF extracted from VEGF and VRM-loaded PLGA microspheres. **P* < 0.05 and ***P* < 0.01.

4 Conclusion

The VRM nanoparticles-loaded PLGA microspheres were successfully developed by microfluidic platforms. A significant improvement in VEGF loading efficacy and release properties was observed by using VRM nanoparticles. The encapsulated VEGF was fully protected from the organic solvent during the fabrication process through the anhydrous R.M. The VRM-loaded PLGA microspheres achieved zero-order controlled release behavior with a highly reduced initial burst. Furthermore, the HUVEC proliferation assay confirmed that the VEGF functionality was fully preserved by R.M. nanoparticles. In conclusion, the VRM nanoparticles-loaded PLGA microspheres show promising potential for long-term VEGF delivery.

5 Acknowledgements

The research reported in this paper was supported by Osteo Science Foundation through Peter Geistlich Award. The authors would like to thank the financial support from this foundation.

References

1 Ugwoke, M, Agu, R, Verbeke, N, and Kinget, R. (2005) *Adv. Drug. Deliv. Rev.* **57**(11), 1640– 1665. https://doi.org/10.1016/j.addr.2005.07.009.

2 Thwala, L. N., Préat, V., and Csaba, N. S. (2017) *Exp. Opin. Drug Deliv.* **14**(1), 23– 36. https://doi.org/10.1080/17425247.2016.1206074.

3 Visser, R., Rico-Llanos, G. A., Pulkkinen, H., and Becerra, J. (2016) *J. Control. Release* **244**, 122– 135. https://doi.org/10.1016/j.jconrel.2016.10.024.

4 Yuan, W., Geng, Y., Wu, F., Liu, Y., Guo, M., Zhao, H., and Jin, T. (2009) *Int. J. Pharm.* **366**(1-2), 154– 159. https://doi.org/10.1016/j.ijpharm.2008.09.007.

5 Chowdhury, M. A. (2016) *Curr. Drug Deliv.* **13**(6), 839– 856. https://doi.org/10.2174/1567201813666151202195104.

6 Place, E. S., Evans, N. D., and Stevens, M. M. (2009) *Nat. Mater.* **8**(6), 457– 470. https://doi.org/10.1038/nmat2441.

7 Folkman, J. (2007) *Nat. Rev. Drug Discov.* **6**(4), 273– 286.

8 Carmeliet, P. (2005) *Nature* **438**, 932– 936.

9 Van Bruggen, N., Thibodeaux, H., Palmer, J. T., Lee, W. P., Fu, L., Cairns, B., Tumas, D., Gerlai, R., Williams, S. P., van Lookeren Campagne, M., and Ferrara, N. (1999) *J. Clin. Invest.* **104**(11), 1613– 1620.
10 Crafts, T. D., Jensen, A. R., Blocher-Smith, E. C., and Markel, T. A. (2015) *Cytokine* **71**, 385– 393.
11 Dashnyam, K., Jin, G. Z., Kim, J. H., Perez, R., Jang, J. H., and Kim, H. W. (2017) *Biomaterials* **116**, 145– 157.
12 Maharaj, A. S. R., and D'Amore, P. A. (2007) *Microvasc. Res.* **74**, 100– 113.
13 List, A. F. (2001) *Oncologist* **6**(5), 24– 31.
14 Zietz, C., Rössle, M., Haas, C., Sendelhofert, A., Hirschmann, A., Stürzl, M., and Löhrs, U. (1998) *Am. J. Pathol.* **153**(5), 1425– 1433.
15 Adamis, A. P., Aiello, L. P., and D'Amato, R. A. (1999) *Angiogenesis* **3**, 9– 14.
16 Ozawa, C. R., Banfi, A., Glazer, N. L., Thurston, G., Springer, M. L., Kraft, P. E., McDonald, D. M., and Blau, H. M. (2004) *J. Clin. Invest.* **113**(4), 516– 527.
17 Simons, M., and Ware, J. A. (2003) *Nat. Rev. Drug Discov.* **2**, 863– 871.
18 da Silva Bitencourt, C., da Silva, L. B., Pereira, P. A. T., Gelfuso, G. M., and Faccioli, L. H. (2015) *Colloids Surf. B Biointerfaces* **136**, 678– 686.
19 Chen, M. M., Cao, H., Liu, Y. Y., Liu, Y., Song, F. F., Chen, J. D., Zhang, Q. Q., and Yang, W. Z. (2017) *Colloids Surf. B Biointerfaces* **151**, 189– 195.
20 Fornaguera, C., Feiner-Gracia, N., Calderó, G., García-Celma, M. J., and Solans, C. (2016) *Colloids Surf. B Biointerfaces* **147**, 201– 209.
21 Sun, L., Liu, Z., Wang, L., Cun, D., Tong, H. H. Y., Yan, R., Chen, X., Wang, R., and Zheng, Y. (2017) *J. Control. Release* **254**, 44– 54.
22 Liu, Z., Zhu, Y., Liu, X., Yeung, K. W. K., and Wu, S. (2017)*Colloids Surf. B Biointerfaces* **151**, 165– 177.
23 Qiao, T., Jiang, S., Song, P., Song, X., Liu, Q., Wang, L., and Chen, X. (2016) *Colloids Surf. B Biointerfaces* **146**, 221– 227.
24 Mir, M., Ahmed, N., and Rehman, A. U. *Colloids Surf. B.* **159**, 217– 231.
25 Omidi, M., Hashemi, M., and Tayebi, L. (2019) *RSC Adv.* **9**(57), 33246– 3356.
26 Guimarães Sá Correia, M., Briuglia, M. L., Niosi, F., and Lamprou, D. A. (2017) *Int. J. Pharm.* **516**(1–2), 91– 99.
27 Maeki, M., Kimura, N., Sato, Y., Harashima, H., and Tokeshi, M. (2018) *Adv. Drug Deliv. Rev.* **128**, 84– 100.
28 Hashemi, M., Yadegari, A., Yazdanpanah, G., Jabbehdari, S., Omidi, M., and Tayebi, L. (2016) *RSC Adv.* **6**(78), 74072– 74084.
29 Omidi, M., Yadegari, A., and Tayebi, L. (2017) *RSC Adv.* **7**(18), 10638– 49.
30 Wentink, M. Q., Broxterman, H. J., Lam, S. W., Boven, E., Walraven, M., Griffioen, A. W., Pili, R., van der Vliet, H. J., de Gruijl, T. D., and Verheul, H. M. W. (2016) *Br. J. Cancer* **115**(8), 940– 948.
31 Huang, Z., Wu, H., Yang, B., Chen, L., Huang, Y., Quan, G., Zhu, C., Li, X., Pan, X., and Wu, C. (2017) *Drug Deliv.* **24**(1), 527– 538.
32 Chen, L., Mei, L., Feng, D., Huang, D., Tong, X., Pan, X., Zhu, C,. and Wu, C. (2018) *Colloids Surf. B Biointerfaces* **163**, 146– 154.
33 Taluja, A., Youn, Y. S., and Bae, Y. H. (2007) *J. Mater. Chem.* **17**(38), 4002– 4014.
34 Pessi, J., Santos, H. A., Miroshnyk, I., Yliruusi, J., Weitz, D. A., and Mirza, S. (2014) *Int. J. Pharm.* **472**(1–2), 82– 87.
35 Sanjay, S. T., Zhou, W., Dou, M., Tavakoli, H., Ma, L., Xu, F., Le, X. (2018) *Adv. Drug Deliv. Rev.* **128**, 3– 28.
36 King, T. W., and Patrick, C. W. (2000) *J. Biomed. Mater. Res.* **51**(3), 383– 390.

37 Raman, C., Berkland, C., Kim, K., and Pack, D. W. (2005) *J. Control. Release.* **103**(1), 149– 158.
38 Golub, J. S., Kim, Y. T., Duvall, C. L., Bellamkonda, R. V., Gupta, D., Lin, A. S., Weiss, D., Robert Taylor, W., and Guldberg, R. E. (2010) *Am. J. Physiol. – Hear. Circ. Physiol.* **298**(6), H1959– H1965.
39 Karal-Yılmaz, O., Serhatlı, M., Baysal, K., and Baysal, B. M. (2011) *J. Microencapsul.* **28**(1), 46– 54.
40 Simón-Yarza, T., Formiga, F. R., Tamayo, E., Pelacho, B., Prosper, F., and Blanco–Prieto, M. J. (2013) *Int. J. Pharm.* **440**(1), 13– 18.
41 Rui, J., Dadsetan, M., Runge, M. B., Spinner, R. J., Yaszemski, M. J., Windebank, A. J., and Wang, H. (2012) *Acta. Biomater.* **8**(2), 511– 518.
42 Yadav, A. K., Mishra, P., Mishra, A. K., Mishra, P., Jain, S., and Agrawal, G. P. (2007) *Nanomedicine Nanotechnology, Biol Med.* **3**(4), 246– 257.
43 Diwan, M., and Park, T. G. (2001) *J. Control Release* **73**(23), 233– 244.
44 Klose, D., Siepmann, F., Elkharraz, K., and Siepmann, J. (2008) *Int. J. Pharm.* **354**(1-2), 95– 103.
45 Siepmann, J., Faisant, N., Akiki, J., Richard, J., and Benoit, J. P. (2004) *J. Control Release* **96**(1), 123– 134.